

Ground-State Thermodynamics of Bistable Redox-Active Donor–Acceptor Mechanically Interlocked Molecules

ALBERT C. FAHRENBACH, CARSON J. BRUNS, DENNIS CAO, AND
J. FRASER STODDART*

Department of Chemistry, Northwestern University, 2145 Sheridan Road, Evanston, Illinois 60208-3113, United States, and NanoCentury KAIST Institute, Graduate School of Energy, Environment, Water, and Sustainability (World Class University), Korea Advanced Institute of Science and Technology (KAIST), 373-1 Guseong Dong, Yuseong Gu, Daejeon 305-701, Republic of Korea

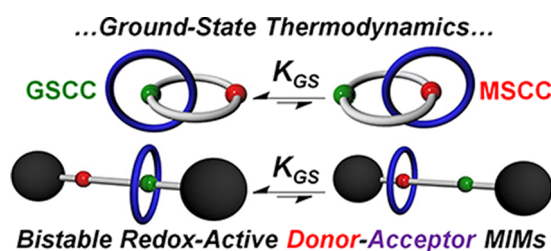
RECEIVED ON MARCH 1, 2012

CONSPECTUS

Fashioned through billions of years of evolution, biological molecular machines, such as ATP synthase, myosin, and kinesin, use the intricate relative motions of their components to drive some of life's most essential processes. Having control over the motions in molecules is imperative for life to function, and many chemists have designed, synthesized, and investigated artificial molecular systems that also express controllable motions within molecules. Using bistable mechanically interlocked molecules (MIMs), based on donor–acceptor recognition motifs, we have sought to imitate the sophisticated nanoscale machines present in living systems. In this Account, we analyze the thermodynamic characteristics of a series of redox-switchable [2]rotaxanes and [2]catenanes. Control and understanding of the relative intramolecular movements of components in MIMs have been vital in the development of a variety of applications of these compounds ranging from molecular electronic devices to drug delivery systems.

These bistable donor–acceptor MIMs undergo redox-activated switching between two isomeric states. Under ambient conditions, the dominant translational isomer, the ground-state coconformation (GSCC), is in equilibrium with the less favored translational isomer, the metastable-state coconformation (MSCC). By manipulating the redox state of the recognition site associated with the GSCC, we can stimulate the relative movements of the components in these bistable MIMs.

The thermodynamic parameters of model host–guest complexes provide a good starting point to rationalize the ratio of GSCC to MSCC at equilibrium. The bistable [2]rotaxanes show a strong correlation between the relative free energies of model complexes and the ground-state distribution constants (K_{GS}). This relationship does not always hold for bistable [2]catenanes, most likely because of the additional steric and electronic constraints present when the two rings are mechanically interlocked with each other. Measuring the ground-state distribution constants of bistable MIMs presents its own set of challenges. While it is possible, in principle, to determine these constants using NMR and UV–vis spectroscopies, these methods lack the sensitivity to permit the determination of ratios of translational isomers greater than 10:1 with sufficient accuracy and precision. A simple application of the Nernst equation, in combination with variable scan-rate cyclic voltammetry, however, allows the direct measurement of ground-state distribution constants across a wide range ($K_{GS} = 10–10^4$) of values.



Introduction

The motions of molecules, small though they may be, impact us in our everyday lives in significant ways. The kinetic energy resulting from the motions of single molecules with random trajectories in an ensemble is detected¹ as temperature, and at the most fundamental level of life,

molecular motions are what keep biological organisms warm and supplied with the energy essential for living. Indeed, the collective motion of molecules can drive objects many orders of magnitude more massive than the molecules themselves into random jittering, known² as Brownian motion. In contrast to these random motions, billions

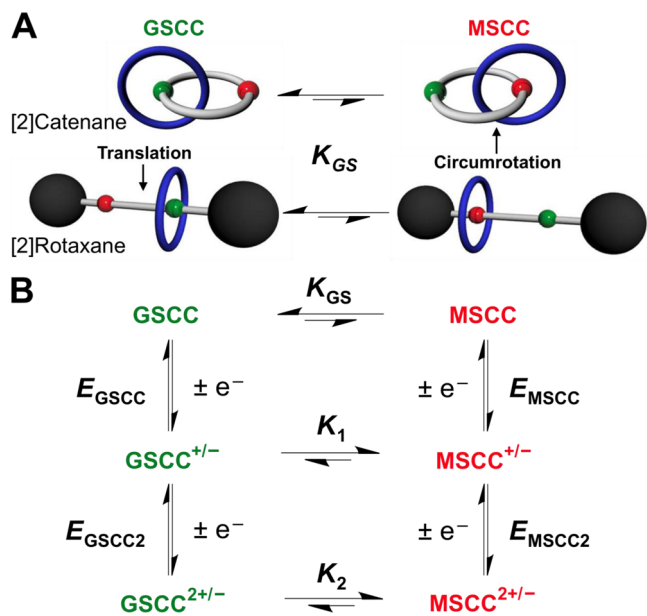


FIGURE 1. General mechanisms for controlled mechanical motions in bistable, redox-active donor–acceptor MIMs. (A) Graphical representations of the two coconformational isomers present in the ground-state distributions of [2]catenanes and [2]rotaxanes. (B) A generalized scheme of equilibration between the GSCC and MSCC as oxidative or reductive stimuli are applied.

of years of evolution have yielded highly sophisticated biological molecular machines, for example, ATP synthase,³ myosin,⁴ and kinesin,⁵ which demonstrate exquisite control in the relative molecular motions of their components and, with it, the ability to do meaningful work on their environments. Having control over the motions of molecules is no doubt imperative in order for life to function, and a significant amount of research^{6–10} has been carried out in the chemical community to design, synthesize, and investigate artificial molecular systems that also express controllable molecular motions. Toward this end, we have focused on artificial molecular systems in the form of bistable mechanically interlocked molecules¹¹ (MIMs), which, by their inherent nature, offer a rich platform to investigate different ways to control^{12–14} the relative motions that interconvert these bistable MIMs between their two different coconformations.¹⁵ The acquisition of control over intramolecular mechanical motions in MIMs not only is important in the context of understanding of how biological molecular machines work but also has led to the invention of a variety of potential applications.^{16–21}

One of the most common examples of bistable MIMs comes in the form of redox-active donor–acceptor [2]rotaxanes and [2]catenanes. A [2]rotaxane consists of a macrocyclic ring mechanically interlocked around a dumbbell-shaped

component, while a [2]catenane is composed of two mechanically interlocking rings (Figure 1A). The noncovalent donor–acceptor interactions that occur when π -electron-rich guests and π -electron-poor hosts (or vice versa) are brought together in solution have been exploited²² in the template-directed synthesis of MIMs for well over two decades. These donor–acceptor interactions, often aided and abetted²³ by [C–H \cdots O] and [C–H \cdots π] noncovalent bonding interactions, “live on” in the MIMs, and they can be nullified or even completely inverted in many cases, by making use of redox chemistry. The key design strategy for bistability in these donor–acceptor redox-active MIMs relies on the incorporation of an additional recognition site in the dumbbell (for rotaxanes) or ring (for catenanes), to which the degenerate ring can translocate following oxidation or reduction of the redox-active recognition unit. These two different translational isomers, also known as coconformations, coexist in the ground state at equilibrium according to a distribution that is governed by the difference in free energy between the coconformations. The mechanistic, structural, and electronic parameters that influence the ground-state distribution of coconformations are some of the most important design elements that need to be understood in order to attain precise control over the redox-induced relative molecular motions that arise in these bistable donor–acceptor MIMs. Intimate mechanistic knowledge of the ground-state distribution of coconformations, in particular, the ability to measure²⁴ their thermodynamic distribution constants, offers one of the keys to controlling molecular mechanical motions from a thermodynamic perspective and provides one piece of the blueprint for designing a MIM to fit the demands of a given function.

In this Account, we review the thermodynamic characteristics that underpin a variety of bistable redox-active donor–acceptor MIMs that have been undergoing development during the past 15 years. Herein, we will (i) formally introduce the redox-stimulated mechanism of switching, universal to all of the bistable MIMs covered in this Account, (ii) discuss pertinent supramolecular species as model systems in the context of their predictive and explanatory powers regarding the ground-state thermodynamics of the bistable MIMs, (iii) summarize the available methods for measuring their ground-state distribution constants directly at equilibrium, (iv) highlight the ground-state thermodynamics of a few selected examples of these bistable MIMs reported in the literature, and (v) compile the binding constants of relevant host–guest complexes and ground-state distribution constants for a variety of different bistable redox-active donor–acceptor MIMs.

A Universal Mechanism at Work

A generalized electrochemical mechanism of switching (Figure 1B) describes the performance of all the bistable MIMs reviewed in this Account. The dominant translational isomer, that is, the most thermodynamically stable one, is typically referred to²⁵ as the ground-state coconformation (GSCC), while the other isomer is deemed the metastable-state coconformation (MSCC). Oxidation or reduction of the donor or acceptor unit encircled by the ring in the GSCC leads to a situation where the ring's affinity for this unit is lost and in many cases further destabilized by Coulombic forces causing the ring to migrate toward the alternative recognition unit. As a consequence of the electronic nature of donor–acceptor interactions, which lower²⁶ the energy of the HOMO centralized on

the donor and raise the energy of the LUMO centralized on the acceptor, the position of the ring can therefore be inferred by noting any shifts in the values of the redox potentials. It is important to note that this mechanism of switching assumes that once the ring translocates to the alternative recognition site, it is no longer influenced electronically by the oxidized or reduced unit it formerly encircles. Consequently, the redox potential of the second one-electron redox process typical to these donor or acceptor units will be very close to that of the corresponding free unit, providing a way to probe the position of the ring after the first redox stimulus. Reversal of the stimulus by reduction or oxidation of the redox-active site back to its original state eventually yields the GSCC/MSCC ground-state distribution that was present at the outset.

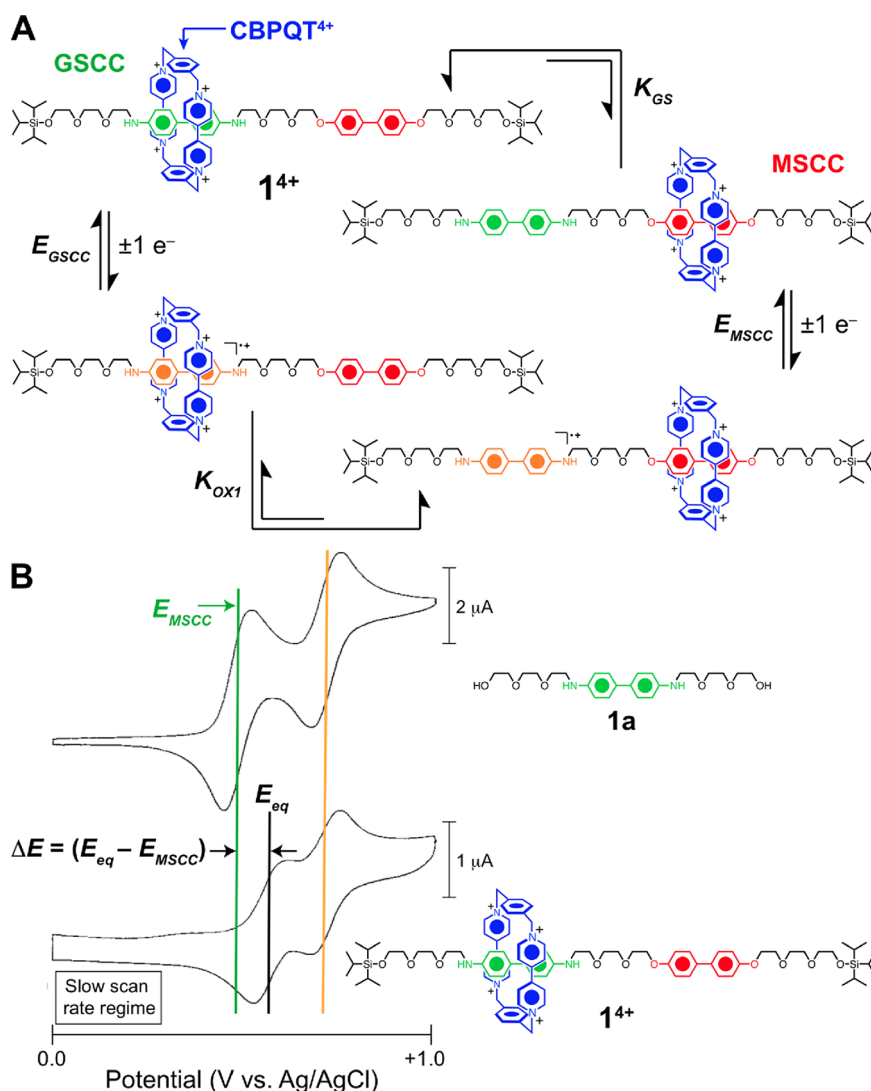


FIGURE 2. The redox-active donor–acceptor bistable [2]rotaxane molecular switch 1^{4+} . (A) Mechanism reflecting redox control over the distribution of coconformations. One-electron oxidation of the primary benzidine recognition unit yields a species in which the secondary biphenol recognition unit is preferentially encircled by the CBPQT⁴⁺ ring. (B) Cyclic voltammograms (0.1 M TBAPF₆/MeCN, 298 K, 100 mV · s⁻¹) of derivative **1a** as a control and 1^{4+} , showing the appearance of E_{eq} for 1^{4+} in the slow-scan-rate regime.

We now discuss a specific example of this electrochemical mechanism of switching by considering the first bistable redox-active donor–acceptor [2]rotaxane **1**⁴⁺ reported²⁷ by us in 1994. This rotaxane is composed (Figure 2A) of the electron-poor cyclophane cyclobis(paraquat-*p*-phenylene) (CBPQT⁴⁺) and a dumbbell containing electron-rich 4,4'-diaminobiphenyl (benzidine) and 1,1'-dioxy-4,4'-biphenylene (biphenol) recognition units. Investigations relying upon ¹H NMR spectroscopic analysis (CD₃CN, 229 K) revealed that encirclement of the CBPQT⁴⁺ ring around either the benzidine or the biphenol units is distributed in a ratio of 84:16, respectively, at equilibrium. Hence, in the case of **1**⁴⁺, the GSCC is the translational isomer in which the CBPQT⁴⁺ ring encircles the benzidine unit. A one-electron oxidation of the benzidine unit to its radical cation introduces a repulsive Coulombic force, which causes the ring to shuttle to the biphenol unit. The value of the potential of this redox process was observed (Figure 2B) by cyclic voltammetry (CV) to be shifted positively compared with the first oxidation of the control benzidine compound **1a**, providing yet another indication experimentally that the CBPQT⁴⁺ ring favors the benzidine station in the ground state. The value of the redox potential for the second redox process of the benzidine unit in **1**⁴⁺ that furnishes the dication is almost identical to that for **1a**, an observation that indicates that the CBPQT⁴⁺ ring must be encircling the biphenol unit predominantly, following the first oxidation process. The return scan of the CV shows that both of these redox processes are reversible and reduction of benzidine back to its neutral form leads to the original ground-state distribution.

Supramolecular Precursors as Thermodynamic Models

In order to rationalize the ground-state distributions in the bistable MIMs, we can turn to host–guest chemistry to provide answers. We reasoned that the binding affinity of the CBPQT⁴⁺ ring for benzidine-containing guests must be approximately an order of magnitude larger than that for biphenol-containing guests and that these relative differences in affinity are preserved in the case of the bistable [2]rotaxane. Indeed, measurements of the binding constants for tri(ethylene glycol) functionalized derivatives of benzidine and biphenol reveal²⁸ values of 800 ± 87 and $104 \pm 13 \text{ M}^{-1}$, respectively. These investigations mark the beginnings of a design strategy that looks to the differences in binding energies between pairs of recognition units with a particular host in order to gain predictive insight into the thermodynamic ground-state behavior of these types of functional molecular switches.

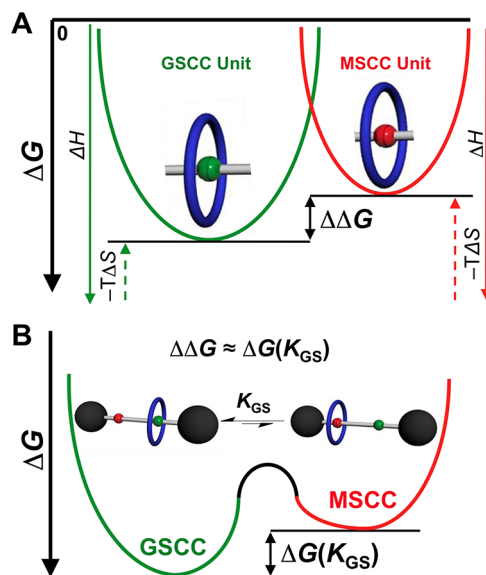
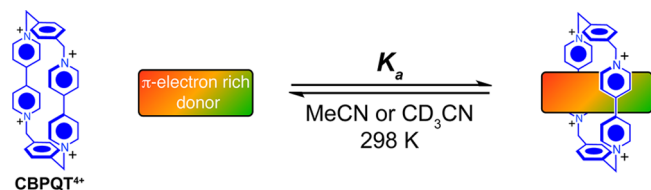


FIGURE 3. Reaction coordinate diagrams of (A) pseudorotaxanes and (B) the corresponding bistable MIMs employing the same recognition motifs, with the relevant thermodynamic parameters $\Delta\Delta G$, ΔH , $T\Delta S$, and $\Delta G(K_{GS})$ defined.

The strategy can be generalized with the assistance²⁹ (Figure 3) of reaction coordinate diagrams. Given a particular ring, the free energies of binding for two different guests are measured and compared. The difference in these binding energies offers a reasonably quantitative prediction of the ground-state distribution of a bistable MIM that incorporates these recognition units. For example, if a 10:1 distribution of GSCC to MSCC is desired, then the difference in the free energy of binding between two different guests with a particular ring of approximately $-1.6 \text{ kcal mol}^{-1}$ should be sought. Additional noncovalent bonding interactions, other than those of the π -donor–acceptor ilk, however, often need to be considered when taking these comparisons into consideration. In particular, [C–H···O] interactions between polyethers and electron-deficient (acidic) aromatic protons play an important role in organic solvents, especially¹⁵ nonpolar ones. In some instances, these additional interactions can increase³⁰ binding constants by up to two orders of magnitude. (see Table 1).^{31–37} The addition of oligo(ethylene glycol) chains, however, does not always lead to significant increases in binding affinities. The binding affinities of benzidine and biphenol with the CBPQT⁴⁺ ring are approximately the same as those of their tri(ethylene glycol) functionalized counterparts. These observations point to a need for careful scrutiny of the subtle interplay between π -associated donor–acceptor and [C–H···O] interactions that must be taken into consideration when designing a bistable MIM.

Using the thermodynamic properties of host–guest complexes (Tables 1 and 2)^{38–41} as models works well in many

TABLE 1. Association Constants (K_a) and Free Energies of Association (ΔG_a) at 298 K in MeCN/CD₃CN of Some Donor–Acceptor Pseudorotaxanes Based on the CBPQT⁴⁺ Ring Employed in the Construction of Bistable Redox-Active Donor–Acceptor MIMs



Entry	Donor Structure	K_a (M ⁻¹)	$-\Delta G_a$ (kcal·mol ⁻¹)	Method ^a	Ref
1		6900	5.2	ITC	30
		7200	5.3	NMRD	31
		8000	5.3	ST	31
		10000	5.5	NMRT	32
2		380000	7.6	ITC	30
3		8580	5.4	ITC	33
4		70800	6.6	ITC	30
5		168000	7.1	ITC	30
6		1040	4.1	ST	28
7		1100	4.1	ST	34
8		18	1.7	ST	35
9		2200	4.6	NMRCV	36
		3400	4.8	ST	35
10		1070	4.1	NMRT	37
11		770	3.9	ST	35
		440	3.6	ITC	30
12		25400	6.0	ST	35
		36400	6.2	ITC	30
13		140	2.9	ST	28
14		104	2.7	ST	28

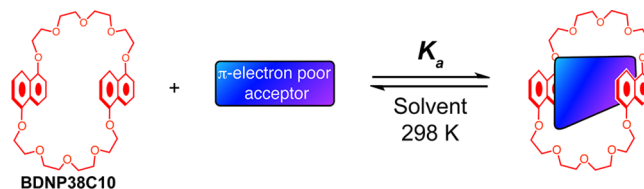
^aMethod abbreviations: ITC = isothermal titration calorimetry, NMRD = NMR dilution method, NMRT = NMR titration method, NMRCV = NMR continuous variation method, ST = spectrophotometric titration.

cases for predicting the ground-state thermodynamic behavior of bistable [2]rotaxanes that incorporate them into their structures. For example, consider **2**⁴⁺, which is composed (Figure 4) of the CBPQT⁴⁺ ring mechanically interlocked around a dumbbell component incorporating TTF and 1,5-dioxynaphthalene (DNP) donor-recognition units linked together by di(ethylene glycol) chains. The free energies of binding (MeCN, 298 K) associated with inclusion of di(ethylene glycol) substituted TTF and DNP derivatives inside the cavity of the CBPQT⁴⁺ ring were measured by ITC and found to be -7.66 ± 0.07 and -6.26 ± 0.04 kcal mol⁻¹, respectively. This difference of 1.4 kcal mol⁻¹ leads to the prediction that in the GSCC of **2**⁴⁺, the CBPQT⁴⁺ ring will

encircle the TTF unit in about a 9:1 ratio with the MSCC where the ring encircles the DNP unit. The predictions are indeed supported by the experimental findings.

The reason that the thermodynamics of host–guest complexes work well in predicting the behavior in bistable [2]rotaxanes is most likely a consequence of the flexible nature of the dumbbell component, which leads to a very similar set of noncovalent bonding interactions as are found in its supramolecular precursors. When applying this predictive strategy in the case of bistable [2]catenanes, however, the geometric constraints imposed by the topology of a catenane in many cases influence the strengths of the various noncovalent bonding interactions and lead to substantial differences (*vide infra*) in the ground-state thermodynamic behavior, defying semiquantitative predictions. The ability to measure the ground-state distributions directly, especially in bistable [2]catenanes, is therefore crucial in order to delineate their thermodynamic behavior, which is not so easily predicted from the analysis of analogous supramolecular model systems.

TABLE 2. Association Constants (K_a) and Free Energies of Association (ΔG_a) at 298 K in Various Solvents of Some Donor–Acceptor Pseudorotaxanes Based on the BDNP38C10 Macrocycle Employed in the Construction of Bistable Redox-Active Donor–Acceptor MIMs



Entry	Acceptor Structure	Solvent	K_a (M ⁻¹)	$-\Delta G_a$ (kcal·mol ⁻¹)	Method ^a	Ref
1		CD ₃ CN	1190	4.2	ST	36
		CD ₃ CN	670	3.8	ST	38
		DMF	29	2.0	ST	39
2		CD ₃ CN	11000	5.5	NMRD	38
3		CD ₃ CN	290000	7.4	ST	38
4		CHCl ₃ /MeOH (98:2)	100	2.7	ITC	40
5		DMF	33	2.1	ST	39
6		CHCl ₃ /MeOH (98:2)	21	1.8	ITC	41

^aMethod abbreviations: ITC = isothermal titration calorimetry, NMRD = NMR dilution method, ST = spectrophotometric titration.

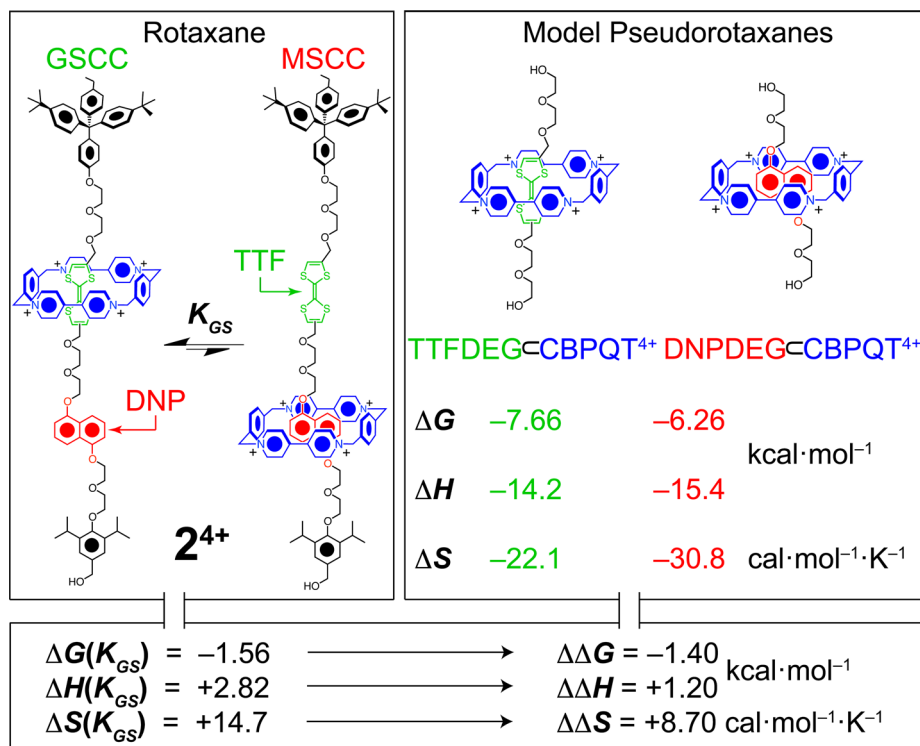


FIGURE 4. Comparison between the thermodynamic parameters characterizing the TTF/DNP bistable [2]rotaxane 2^{4+} and the corresponding pseudorotaxanes TTFDEG-CBPQT $^{4+}$ and DNPDEG-CBPQT $^{4+}$. The $\Delta\Delta G$, $\Delta\Delta H$, and $\Delta\Delta S$ values obtained from the pseudorotaxanes correspond well with ΔG , ΔH , and ΔS values for the ground-state distribution in the bistable rotaxane.

Applying the Formula

The ability to measure the ground-state distribution constants governing the thermodynamic properties of bistable donor–acceptor MIMs directly has been a challenge in the field from its very beginnings. Part of the reason for this challenge is the fact that these MIMs are *single molecules*, and for this reason the same approaches used to evaluate the binding constants of their supramolecular precursors cannot be employed at the molecular level. While ^1H NMR spectroscopy can be a valuable tool for estimating the GSCC/MSCC ratios by measuring the relative intensities of respective proton resonances, this approach has some fundamental limitations. For example, a lack of sensitivity, that is, the ability to distinguish signals originating from the MSCC from those of baseline impurities, often makes it difficult to estimate the distributions for bistable MIMs with ratios exceeding approximately 10:1. In addition to ^1H NMR (but not exceeding its limitations), we have employed CV to measure³⁰ ground-state distribution constants of a number of bistable rotaxanes. This particular electrochemical technique has only enough sensitivity, however, to be applied in the case of bistable MIMs with ground-state distribution constants of 10:1 or less. The point we wish to make here is that developing²⁴ a method for measuring beyond this 10:1 range of sensitivity has been a major challenge.

Only after many years of investigating the collective behavior of a wide variety of these redox-active bistable donor–acceptor MIMs have we been able quite recently to develop a method that can deliver a level of precision that exceeds the 10:1 range of sensitivity. The key concept behind the development of this method, which also employs CV, lies in recognizing that there are two different kinetic regimes with respect to the shuttling of the ring that interconvert the MSCC to GSCC and the scan rate employed in the experiment. The existence of two different kinetic regimes is very similar conceptually to the fast- and slow-exchange regimes that characterize dynamic ^1H NMR spectroscopy. Shuttling of the ring, which interconverts the MSCC and GSCC, can also be either fast or slow on the time scale of the CV experiment. In keeping with this conceptual framework, we employ the terminologies “fast-scan-rate regime” and “slow-scan-rate regime”, the ranges of which depend on the specific kinetics associated with shuttling motion of the ring that vary from one bistable MIM to another. Transition from the fast-scan-rate regime to the slow-scan-rate regime in the case of variable-scan-rate CV can also provide quantitative information of a *thermodynamic* nature, with respect to the ground-state distributions of bistable MIMs.

Consider the following analysis. We can define the equilibrium based upon the ground state distribution between the GSCC and the MSCC for any particular bistable MIM as



where K_{GS} is the ground state distribution constant governing the equilibrium between the GSCC and the MSCC. It is important to note that this analysis is made on the assumption that the unit encircled by the ring in the GSCC is the redox-active unit controlling the switching behavior. We recall that substantial differences in the redox potentials of the donor or acceptor unit associated with the GSCC exist. Therefore, the first redox potential of the recognition unit associated with the GSCC, when encircled by the ring, is much higher than when it is not encircled, as in the case of the MSCC. With this knowledge in hand, consider the following redox equilibrium:



where the plus–minus sign indicates that this equation can be applied to either oxidation or reduction processes. From this relationship, we can invoke the use of the Nernst equation:

$$E_{Ap} = E_{MSCC} \pm \frac{RT}{nF} \ln \left(\frac{[\text{MSCC}^{+/-}]}{[\text{MSCC}]} \right) \quad (3)$$

where E_{MSCC} is the redox potential for the electron transfer process in eq 2, E_{Ap} is the applied potential, R is the universal gas constant, T is the temperature, n is the number of electrons transferred, and F is Faraday's constant. Combining eq 1 with eq 3, we can derive an expression for $[\text{MSCC}]$ in terms of K_{GS} and the $[\text{GSCC}]$.

$$E_{Ap} = E_{MSCC} \pm \frac{RT}{nF} \ln \left(\frac{K_{GS}[\text{MSCC}^{+/-}]}{[\text{GSCC}]} \right) \quad (4)$$

Under the appropriate experimental conditions, where the scan rate is sufficiently slow such that at each point in the scan the redox-stimulated translational motion of the ring is allowed to reach an equilibrium as the potential is varied, there exists an applied potential, E_{Ap} , at which the quantity $([\text{MSCC}^{+/-}]/[\text{GSCC}])$ is equal to unity and effectively defines the new redox potential, call it E_{eq} , which can be observed in the slow-scan-rate regime. Solving eq 4 for K_{GS} leads to the following expression:

$$K_{GS} = \exp \left[(|E_{eq} - E_{MSCC}|) \frac{nF}{RT} \right] \quad (5)$$

Now, we have a means of measuring the ground-state distribution constant K_{GS} as a function of the redox potential

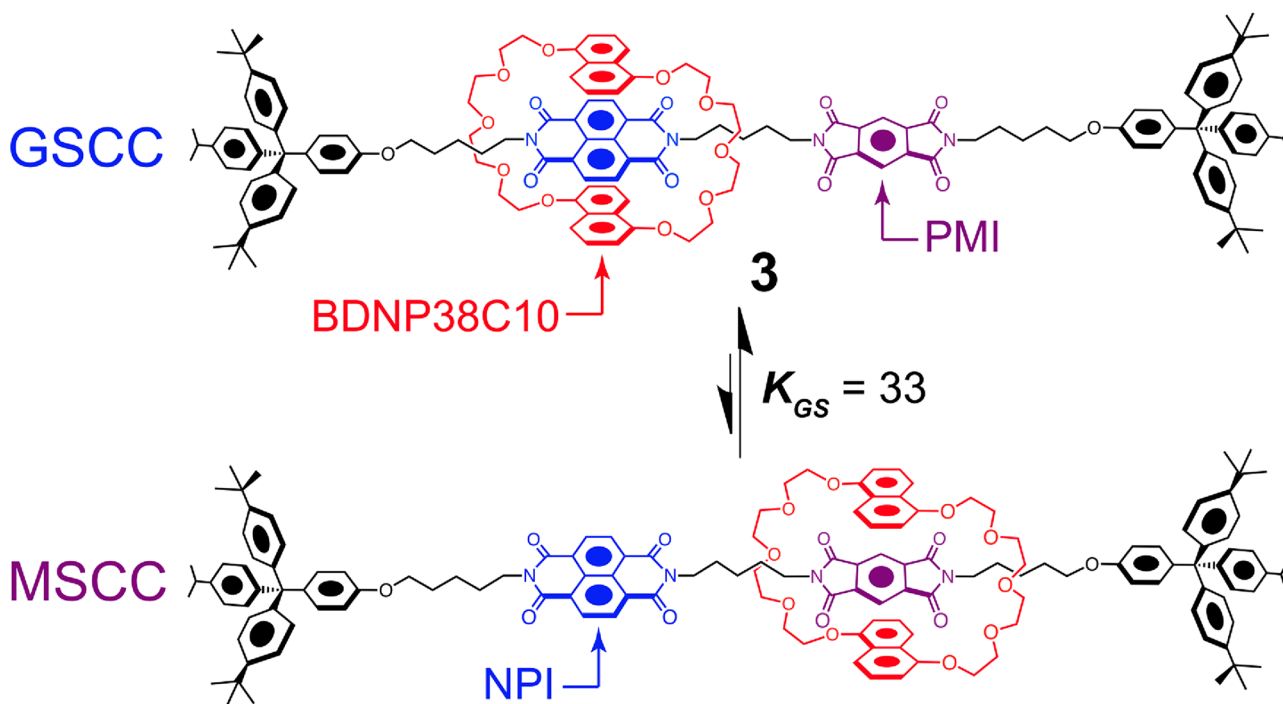


FIGURE 5. Structures of the GSCC and MSCC for the neutral bistable [2]rotaxane **3**. The K_{GS} of 33 that governs the distribution was retrospectively calculated by applying eq 5 to slow-scan-rate CV data.

of E_{eq} and E_{MSCC} for any particular bistable redox-active MIM that obeys the proposed mechanism. In principle, the redox potential E_{MSCC} can be measured directly in the fast-scan-rate regime, while E_{eq} can be obtained in the slow one. If E_{MSCC} cannot be measured directly, then one can rely on the use of a model compound, for example, the free ring or dumbbell components. Furthermore, digitally simulated CV data can be used in comparison to the experimental data in order to determine K_{GS} , and the values determined from this method are the same²⁴ within error when using eq 5.

Let us return now to the example of the benzidene- and biphenol-containing [2]rotaxane **1**⁴⁺. In hindsight, we realize that the CV of the bistable [2]rotaxane was recorded in the slow-scan-rate regime. The potential of the first redox process of the benzidene unit corresponding to E_{eq} is shifted by approximately 60 mV in comparison to the benzidene control compound **1a**, corresponding to E_{MSCC} (Figure 2B). By application of eq 5, this difference of 60 mV leads to a calculated value of $K_{\text{GS}} = 10$, which is in good agreement with the 84 to 16 distribution obtained from ¹H NMR spectroscopy.

In order to demonstrate the general applicability of eq 5, we turn our attention to a neutral bistable donor–acceptor [2]rotaxane **3** (Figure 5) composed⁴² of the electron-rich macrocyclic polyether bis-1,5-dinaphtho[38]crown-10 (BDNP38C10) and a dumbbell incorporating electron-poor naphthalene diimide (NPI) and pyromellitic diimide (PMI) recognition units. The BDNP38C10 ring encircles the NPI unit in the GSCC and the PMI unit in the MSCC. The CV of the rotaxane was recorded (CH₂Cl₂, 298 K) in the slow-scan-rate regime. The first redox couple observed at -0.74 V involves reduction of the NPI unit to its radical anion NPI^{•-}, a redox process that induces translation of the BDNP38C10 ring from the NPI to the PMI unit. Compared with its free dumbbell component, the redox potential for the first reduction of the NPI^{•-} is shifted more negative by 90 mV in the bistable [2]rotaxane **3**. Employing eq 5, we can calculate a ground-state distribution constant K_{GS} of 33, a value that agrees⁴² well with the predicted value. It should be added that the distribution constant for this bistable rotaxane has never been measured directly before now.

In order to illustrate the difference between observing the fast- and slow-scan-rate regimes and how thermodynamic models based on the binding properties of related host–guest compounds do not lead routinely to correct predictions for bistable catenanes, we turn our attention to the example of a [2]catenane **4**⁴⁺ composed⁴³ (Figure 6) of a CBPQT⁴⁺ ring mechanically bonded with a macrocyclic

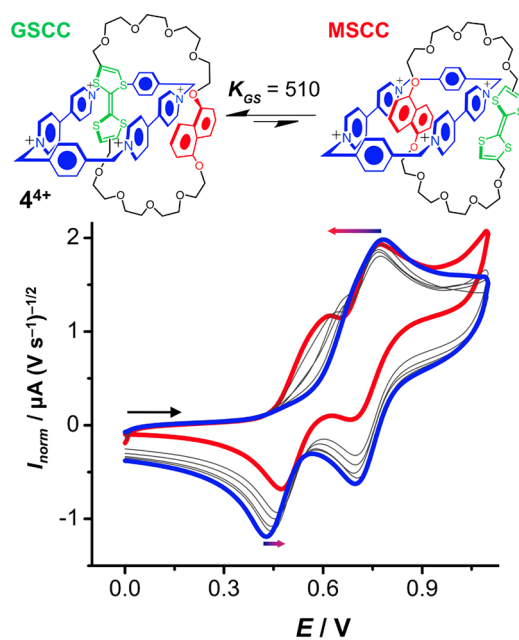


FIGURE 6. Variable-scan-rate cyclic voltammograms for the bistable [2]catenane **4**⁴⁺, showing the transition from a fast-scan-rate regime (blue trace) to a slow-scan-rate regime (red trace). The appearance of E_{eq} at slow scan rates in the CV allows for evaluation of the GSCC/MSCC ratio according to eq 5, revealing a remarkably high equilibrium constant ($K_{\text{GS}} = 510$) in favor of the GSCC.

polyether containing TTF and DNP recognition units. The CVs of **4**⁴⁺ were first reported in the fast-scan-rate regime, shown by the blue trace in Figure 6. As such, the shuttling of the CBPQT⁴⁺ ring from TTF in the GSCC to DNP in the MSCC is slow on the time scale of the experiment. The fact that no oxidation wave is observed around $+0.4$ V, for a process that would provide quantitative information about the distribution constant, means that the ground-state distribution must be greater than 10:1. Only recently, by accessing²⁴ the slow-scan-rate regime for **4**⁴⁺, we were able to measure this distribution constant. By starting out in the fast-scan-rate regime, we found the redox potential E_{MSCC} to be $+0.42$ V. On scanning successively more slowly, we observed a new oxidation process emerge, whose redox potential is $+0.58$ V, corresponding to E_{eq} . Using eq 5, we calculated the ground-state distribution constant to be $K_{\text{GS}} = 510$, which is well over an order of magnitude larger than that predicted from the thermodynamics of the host–guest models. The increased value of K_{GS} in bistable catenanes relative to their rotaxane cousins can be witnessed in other examples. Tables 3 and 4^{44–52} compile ground-state distribution constants for redox-active bistable donor–acceptor MIMs, many of which have not been defined until now, with the retroactive application of eq 5 to their CV data reported in the literature.

TABLE 3. Equilibrium Constants (K_{GS}) Governing the Ground-State Distributions of Various Previously Reported CBPQT⁴⁺-Based Bistable Donor–Acceptor MIMs

Entry	Structure	K_{GS}	Solvent	T (K)	Method ^a	Ref
1		350	MeCN	298	Eqn 5	44
2		23	MeCN	298	Eqn 5	45
3		15	MeCN	298	Eqn 5	24
4	1 ⁴⁺ 	10	MeCN	298	Eqn 5	27
5		10	MeCN	298	CV	46
6	2 ⁴⁺ 	9	MeCN	298	CV	30
7		3	CD ₃ CN	295	NMR	30
8		3	CD ₃ CN	298	NMR	47
9		2	CD ₃ CN	240	NMR	48
10		1	CD ₃ CN	300	NMR	47

^aMethods: “Eqn 5”, eq 5 was applied to the slow-scan-rate CV data reported in the corresponding reference; “NMR”, K_{GS} was measured by comparing integrals of ¹H signals for each coconformation in a slow exchange regime; “CV”, K_{GS} was measured by comparing the integrals of the redox waves corresponding to each coconformation in the fast-scan-rate CV.

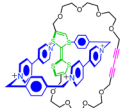

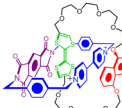
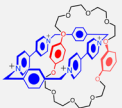
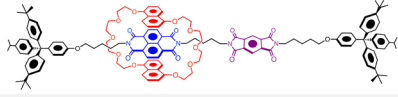
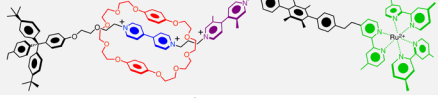
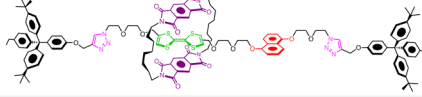
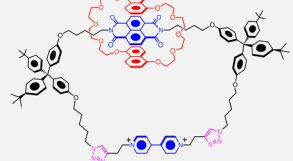
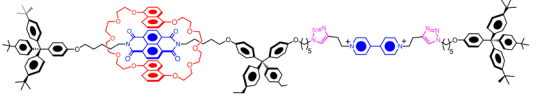

Reflections

As the development of bistable redox-active donor–acceptor MIMs has progressed, a battery of techniques to predict, analyze, and explain their ground-state distributions at equilibrium have been harnessed. Model complexes have proven to be crucial leads in the design of bistable MIMs, and more recently, slow-scan-rate CV has provided the analytical sensitivity required to probe ground-state distribution constants up to 10^4 .

This semiquantitative treatment of the ground-state distributions of coconformations (translational isomers) is

reminiscent of the conformational analysis⁵³ that can be performed on multiply substituted cyclohexane rings once the conformational free energy differences, often referred to as A-values, between equatorial and axial substituents on a monosubstituted cyclohexane ring are known. Although the principle of additivity of A-values cannot be applied universally because of the advent of additional steric (e.g., 1,3-diaxial) and electronic interactions, the approach is generally quite highly predictive, particularly so when allowances are made for the exceptions. The anomeric effect that is present in many carbohydrates⁵⁴ is a good example of an electronic effect that

TABLE 4. Equilibrium Constants (K_{GS}) Governing the Ground State Distributions of Various Previously Reported Crown Ether-Based Bistable Donor–Acceptor MIMs

Entry	Structure	K_{GS}	Solvent	T (K)	Method ^a	Ref
1		11400	MeCN	298	Eqn 5	24
2	4⁴⁺ 	510	MeCN	298	Eqn 5	24
3		340	MeCN	298	Eqn 5	49
4		49	(CD ₃) ₂ CO	253	NMR	37
5	3 	33	CH ₂ Cl ₂	298	Eqn 5	42
6		23	MeCN	298	Eqn 5	50
7		10	Me ₂ CO	298	Eqn 5	51
8		1.5	CD ₃ CN	343	NMR	52
9		1.5	CD ₃ CN	298	NMR	39
10		1	MeCN	298	CV	33

^aMethods: "Eqn 5", eq 5 was applied to the slow-scan-rate CV data reported in the corresponding reference; "NMR", K_{GS} was measured by comparing integrals of ¹H signals for each coconformation in a slow exchange regime; "CV", K_{GS} was measured by comparing the integrals of the redox waves corresponding to each coconformation in the fast-scan-rate CV.

can more than outweigh a steric one in many instances. Nonetheless, it is possible to analyze all the conformational free energies for the 16 D-(α and β)-aldohexopyranoses and then use this information to predict the relative free energies of the eight D-aldohexopyranoses to discover that the three most stable, namely, glucose, mannose, and galactose, also happen to be the most prevalent monosaccharides found in Nature. These kinds of empirically based analyses not only are useful

from the practical viewpoint of the experimentalist but also provide the vehicles for theoreticians to put their ideas to the test. An intimate understanding of the thermodynamic parameters that govern redox-active bistable donor–acceptor MIMs provides one piece of the blueprint for the design of increasingly sophisticated molecules with multiple functionalities, especially in devices, and will provide a means for theory to develop at a level of sophistication where it will be able to

predict quantitatively and with reasonably high certainty the thermodynamic outcome that results from a particular non-covalent bonding pattern present in a given bistable MIM.

We thank the Air Force Office of Scientific Research (AFSOR) for support under the Multidisciplinary Research Program of the University Research Initiative (MURI) Award FA9550-07-1-0534 on "Bioinspired Supramolecular Enzymatic Systems" as well as the National Science Foundation (NSF) for their Award CHE-0924620. We also acknowledge support from the Microelectronics Advanced Research Corporation (MARCO) and its Focus Center Research Program (FCRP) on Functional Engineered NanoArchitectonics (FENA) as well as from the Non-Equilibrium Energy Research Center (NERC), which is an Energy Frontier Research Center (EFRC) funded by the U.S. Department of Energy, Office of Basic Sciences (DOE-BES), under Award DE-SC0000989. A.C.F., C.J.B., D.C., and J.F.S. were all beneficiaries of the WCU Program (NRFR-31-2008-000-10055-0) funded by the Ministry of Education, Science and Technology, Korea. A.C.F., C.J.B., and D.C. acknowledge support from NSF Graduate Research Fellowships.

BIOGRAPHICAL INFORMATION

Albert C. Fahrenbach was born and raised in the United States in rural Indiana. He entered Indiana University of Bloomington in 2003 and received an Honors B.Sc. Degree there in 2008 in Chemistry, while conducting chemical synthesis under the tutelage of Professor Amar Flood. In the same year, Albert moved to Northwestern University to study for his Ph.D. Degree with Professor Fraser Stoddart. The joy associated with the design, synthesis, and investigation of molecular switches and machines is what keeps Albert coming into laboratory early every morning. Enjoying the company of his fellow students is what keeps him in the laboratory late into the night.

Carson J. Bruns grew up in the foothills of the Rocky Mountains in Loveland, Colorado, where he fostered his interests in running, hiking, and camping. He attended Luther College in Decorah, Iowa, with concentrations in chemistry and religion and spent summers researching organic synthesis in two NSF REU programs, advised by Professors Scott Stoudt at Coe College in Cedar Rapids, Iowa, and Nopporn Thasana at Chulabhorn Research Institute in Bangkok, Thailand. After receiving his B.A. in Spring 2008, he joined the Stoddart and Stupp groups at Northwestern University to investigate the self-assembly of exotic interlocked architectures for his Ph.D. degree.

Dennis Cao was born in Konstanz, Germany, and raised in San Diego, CA. He carried out undergraduate research in the Molecular Foundry at the Lawrence Berkeley National Laboratory under the tutelage of Dr. Yi Liu, designing and synthesizing mechanically interlocked molecules, as well as compounds for organic photovoltaic applications. He joined the Stoddart group at Northwestern University in November 2010. Outside of the laboratory, he enjoys sports, photography, and video games.

J. Fraser Stoddart received all (B.Sc., Ph.D., D.Sc.) of his degrees from the University of Edinburgh, U.K. Presently, he holds a Board of Trustees Professorship in the Department of Chemistry at NU. His research has opened up a new materials world of mechanically interlocked molecules and, in doing so, has produced a blueprint for the subsequent growth of functional molecular nanotechnology and the fabrication of functional integrated systems.

FOOTNOTES

*Correspondence address: Department of Chemistry, Northwestern University, 2145 Sheridan Road Evanston, Illinois 60208-3113. Tel: (+1)-847-491-3793. Fax: (+1)-847-491-1009. E-mail: stoddart@northwestern.edu. The authors declare no competing financial interest.

REFERENCES

- Atkins, P.; De Paula, J. *Physical Chemistry*; W. H. Freeman and Co.: New York, 2009.
- Einstein, A. Über die von der Molekular-kinetischen Theorie der Wärme Geforderte Bewegung von in Ruhenden Flüssigkeiten Suspensierten Teilchen. *Ann. Phys.* **1905**, *322*, 549–560.
- Itoh, H.; Takahashi, A.; Adachi, K.; Noji, H.; Yasuda, R.; Yoshida, M.; Kinosita, K. Mechanically Driven ATP Synthesis by F₁-ATPase. *Nature* **2004**, *427*, 465–468.
- Sweeney, H. L.; Houdusse, A. Structural and Functional Insights into the Myosin Motor Mechanism. *Annu. Rev. Biophys.* **2010**, *39*, 539–557.
- van den Heuvel, M. G. L.; Dekker, C. Motor Proteins at Work for Nanotechnology. *Science* **2007**, *317*, 333–336.
- Barrell, M. J.; Campaña, A. G.; von Delius, M.; Geertsema, E. M.; Leigh, D. A. Light-Driven Transport of a Molecular Walker in Either Direction along a Molecular Track. *Angew. Chem., Int. Ed.* **2011**, *50*, 285–290.
- Ruangsupapichat, N.; Pollard, M. M.; Harutyunyan, S. R.; Feringa, B. L. Reversing the Direction in a Light-Driven Rotary Molecular Motor. *Nat. Chem.* **2011**, *3*, 53–60.
- Qu, D. H.; Wang, Q. C.; Tian, H. A Half Adder Based on a Photochemically Driven [2]Rotaxane. *Angew. Chem., Int. Ed.* **2005**, *44*, 5296–5299.
- Hua, Y.; Flood, A. H. Flipping the Switch on Chloride Concentrations with a Light-Active Foldamer. *J. Am. Chem. Soc.* **2010**, *132*, 12838–12840.
- Sauvage, J.-P. Transition Metal-Containing Rotaxanes and Catenanes in Motion: Toward Molecular Machines and Motors. *Acc. Chem. Res.* **1998**, *31*, 611–619.
- Stoddart, J. F. The Chemistry of the Mechanical Bond. *Chem. Soc. Rev.* **2009**, *38*, 1802–1820.
- Balzani, V.; Clemente-León, M.; Credi, A.; Ferrer, B.; Venturi, M.; Flood, A. H.; Stoddart, J. F. Autonomous Artificial Nanomotor Powered by Sunlight. *Proc. Natl. Acad. Sci. U.S.A.* **2006**, *103*, 1178–1183.
- Garandé, S.; Silvi, S.; Venturi, M.; Credi, A.; Flood, A. H.; Stoddart, J. F. Shuttling Dynamics in an Acid-Base Switchable [2]Rotaxane. *Chem. Phys. Chem.* **2005**, *6*, 2145–2152.
- Tseng, H.-R.; Vignon, S. A.; Celestre, P. C.; Perkins, J.; Jeppesen, J. O.; Di Fabio, A.; Ballardini, R.; Gandolfi, M. T.; Venturi, M.; Balzani, V.; Stoddart, J. F. Redox-Controllable Amphiphilic [2]Rotaxanes. *Chem.—Eur. J.* **2004**, *10*, 155–172.
- Fyfe, M. C. T.; Glink, P. T.; Menzer, S.; Stoddart, J. F.; White, A. J. P.; Williams, D. J. Anion-Assisted Self-Assembly. *Angew. Chem., Int. Ed. Engl.* **1997**, *36*, 2068–2070.
- Thordarson, P.; Bijsterveld, E. J. A.; Rowan, A. E.; Nolte, R. J. M. Epoxidation of Polybutadiene by a Topologically Linked Catalyst. *Nature* **2003**, *424*, 915–918.
- Coti, K. K.; Belowich, M. E.; Liong, M.; Ambrogio, M. W.; Lau, Y. A.; Khatib, H. A.; Zink, J. I.; Khoshdel, N. M.; Stoddart, J. F. Mechanised Nanoparticles for Drug Delivery. *Nanoscale* **2009**, *1*, 16–39.
- Fang, L.; Hmadeh, M.; Wu, J.; Olson, M. A.; Spruell, J. M.; Trabolsi, A.; Yang, Y.-W.; Elhabri, M.; Albrecht-Gary, A.-M.; Stoddart, J. F. Acid-Base Actuation of [c2]Daisy Chains. *J. Am. Chem. Soc.* **2009**, *131*, 7126–7134.
- Ito, K. Slide-Ring Materials Using Topological Supramolecular Architecture. *Curr. Opin. Solid State Mater. Sci.* **2010**, *14*, 28–34.
- Berná, J.; Leigh, D. A.; Lubomska, M.; Mendoza, S. M.; Pérez, E. M.; Rudolf, P.; Teobaldi, G.; Zerbetto, F. Macroscopic Transport by Synthetic Molecular Machines. *Nat. Mater.* **2005**, *4*, 704–710.
- Green, J. E.; Choi, J. W.; Boukai, A.; Bunimovich, Y.; Johnston-Halpin, E.; Delonno, E.; Luo, Y.; Sheriff, B. A.; Xu, K.; Shin, Y. S.; Tseng, H.-R.; Stoddart, J. F.; Heath, J. R. A 160-Kilobit Molecular Electronic Memory Patterned at 10¹¹ Bits per Square Centimetre. *Nature* **2007**, *445*, 414–417.
- Griffiths, K. E.; Stoddart, J. F. Template-Directed Synthesis of Donor/Acceptor [2]Catenanes and [2]Rotaxanes. *Pure Appl. Chem.* **2008**, *80*, 485–506.

- 23 Houk, K. N.; Menzer, S.; Newton, S. P.; Raymo, F. M.; Stoddart, J. F.; Williams, D. J. Molecular Meccano. Part 47. [C-H...O] Interactions as a Control Element in Supramolecular Complexes: Experimental and Theoretical Evaluation of Receptor Affinities for the Binding of Bipyridinium-Based Guests by Catenated Hosts. *J. Am. Chem. Soc.* **1999**, *121*, 1479–1487.
- 24 Fahrenbach, A. C.; Barnes, J. C.; Li, H.; Benítez, D.; Basuray, A. N.; Fang, L.; Sue, C.-H.; Barin, G.; Dey, S. K.; Goddard, W. A., III; Stoddart, J. F. Measurement of the Ground-State Distributions in Bistable Mechanically Interlocked Molecules Using Slow Scan Rate Cyclic Voltammetry. *Proc. Natl. Acad. Sci. U.S.A.* **2011**, *108*, 20416–20421.
- 25 Flood, A. H.; Peters, A. J.; Vignon, S. A.; Steuerman, D. W.; Tseng, H.-R.; Kang, S.; Heath, J. R.; Stoddart, J. F. The Role of Physical Environment on Molecular Electromechanical Switching. *Chem.—Eur. J.* **2004**, *10*, 6558–6564.
- 26 Veldman, D.; Meskers, S. C. J.; Janssen, R. A. J. The Energy of Charge-Transfer States in Electron Donor–Acceptor Blends: Insight into the Energy Losses in Organic Solar Cells. *Adv. Funct. Mater.* **2009**, *19*, 1939–1948.
- 27 Bissell, R. A.; Córdova, E.; Kaifer, A. E.; Stoddart, J. F. A Chemically and Electrochemically Switchable Molecular Device. *Nature* **1994**, *369*, 133–137.
- 28 Córdova, E.; Bissell, R. A.; Spencer, N.; Ashton, P. R.; Stoddart, J. F.; Kaifer, A. E. Novel Rotaxanes Based on the Inclusion Complexation of Biphenyl Guests by Cyclobis(paraquat-p-phenylene). *J. Org. Chem.* **1993**, *58*, 6550–6552.
- 29 Olson, M. A.; Braunschweig, A. B.; Ikeda, T.; Fang, L.; Trabolsi, A.; Slawin, A. M. Z.; Khan, S. I.; Stoddart, J. F. Thermodynamic Forecasting of Mechanically Interlocked Switches. *Org. Biomol. Chem.* **2009**, *7*, 4391–4405.
- 30 Choi, J. W.; Flood, A. H.; Steuerman, D. W.; Nygaard, S.; Braunschweig, A. B.; Moonen, N. N. P.; Laursen, B. W.; Luo, Y.; Delonno, E.; Peters, A. J.; Jeppesen, J. O.; Xe, K.; Stoddart, J. F.; Heath, J. R. Ground-State Equilibrium Thermodynamics and Switching Kinetics of Bistable [2]Rotaxane Switches in Solution, Polymer Gels, and Molecular Electronic Devices. *Chem.—Eur. J.* **2006**, *12*, 261–279.
- 31 Anelli, P.-L.; Asakawa, M.; Ashton, P. R.; Bissell, R. A.; Clavier, G.; Górski, R.; Kaifer, A. E.; Langford, S. J.; Matternsteig, G.; Menzer, S.; Philp, D.; Slawin, A. M. Z.; Spencer, N.; Stoddart, J. F.; Tolley, M. S.; Williams, D. J. Toward Controllable Molecular Shuttles. *Chem.—Eur. J.* **1997**, *3*, 1113–1135.
- 32 Ashton, P. R.; Balzani, V.; Becher, J.; Credi, A.; Fyfe, M. C. T.; Matternsteig, G.; Menzer, S.; Nielsen, M. B.; Raymo, F. M.; Stoddart, J. F.; Venturi, M.; Williams, D. J. A Three-Pole Supramolecular Switch. *J. Am. Chem. Soc.* **1999**, *121*, 3951–3957.
- 33 Wang, C.; Cao, D.; Fahrenbach, A. C.; Fang, L.; Olson, M. A.; Friedman, D. C.; Basu, S.; Dey, S. K.; Botros, Y. Y.; Stoddart, J. F. Solvent-Dependent Ground-State Distributions in a Donor–Acceptor Redox-Active Bistable [2]Catenane. *J. Phys. Org. Chem.* **2012**, *25*, 544–552.
- 34 Córdova, E.; Bissell, R. A.; Kaifer, A. E. Synthesis and Electrochemical Redox Properties of Redox-Active [2]Rotaxanes Based on the Inclusion Complexation of 1,4-Phenylenediamine and Benzidine by Cyclobis(paraquat-p-phenylene). *J. Org. Chem.* **1995**, *60*, 1033–1038.
- 35 Castro, R.; Nixon, K. R.; Evansek, J. D.; Kaifer, A. E. Effects of Side Arm Length and Structure of Para-Substituted Phenyl Derivatives on Their Binding to the Host Cyclobis(paraquat-p-phenylene). *J. Org. Chem.* **1996**, *61*, 7298–7303.
- 36 Asakawa, M.; Ashton, P. R.; Boyd, S. E.; Brown, C. L.; Gillard, R. E.; Kocian, O.; Raymo, F. M.; Stoddart, J. F.; Tolley, M. S.; White, A. J. P.; Williams, D. J. Molecular Meccano 11. Recognition of Bipyridinium-Based Derivatives by Hydroquinone- and/or Dioxynaphthalene-Based Macrocyclic Polyethers - From Inclusion Complexes to the Self-Assembly of [2]Catenanes. *J. Org. Chem.* **1997**, *62*, 26–37.
- 37 Amabilino, D. B.; Anelli, P.-L.; Ashton, P. R.; Brown, G. R.; Córdova, E.; Godínez, L.; Hayes, W.; Kaifer, A. E.; Philp, D.; Slawin, A. M. Z.; Spencer, N.; Stoddart, J. F.; Tolley, M. S.; Williams, D. J. Constitutional and Translational Isomerism in [2]Catenanes and [n]Pseudorotaxanes. *J. Am. Chem. Soc.* **1995**, *117*, 11142–11170.
- 38 Ashton, P. R.; Boyd, S. E.; Brindle, A.; Langford, S. J.; Menzer, S.; Pérez-García, L.; Preece, J. A.; Raymo, F. M.; Spencer, N.; Stoddart, J. F.; White, A. J. P.; Williams, D. J. Molecular Meccano. Part 50. Diazapyrenium-Containing Catenanes and Rotaxanes. *New J. Chem.* **1999**, *23*, 587–602.
- 39 Dey, S. K.; Coskun, A.; Fahrenbach, A. C.; Barin, G.; Basuray, A. N.; Trabolsi, A.; Botros, Y. Y.; Stoddart, J. F. A Redox-Active Reverse Donor-Acceptor Bistable [2]Rotaxane. *Chem. Sci.* **2011**, *2*, 1046–1053.
- 40 Pascu, S. I.; Naumann, C.; Kaiser, G.; Bond, A. D.; Sanders, J. K. M.; Jarrosson, T. Structures and Solution Dynamics of Pseudorotaxanes Mediated by Alkali-Metal Cations. *Dalton Trans.* **2007**, 3874–3884.
- 41 Pascu, S. I.; Jarrosson, T.; Naumann, C.; Otto, S.; Kaiser, G.; Sanders, J. K. M. Cation-Reinforced Donor-Acceptor Pseudorotaxanes. *New J. Chem.* **2005**, *29*, 80–89.
- 42 Iijima, T.; Vignon, S. A.; Tseng, H.-R.; Jarrosson, T.; Sanders, J. K. M.; Marchioni, F.; Venturi, M.; Apostoli, E.; Balzani, V.; Stoddart, J. F. Controllable Donor-Acceptor Neutral [2]Rotaxanes. *Chem.—Eur. J.* **2004**, *10*, 6375–6392.
- 43 Asakawa, M.; Ashton, P. R.; Balzani, V.; Credi, A.; Hamers, C.; Matternsteig, G.; Montalti, M.; Shipway, A. N.; Spencer, N.; Stoddart, J. F.; Tolley, M. S.; Venturi, M.; White, A. J. P.; Williams, D. J. A Chemically and Electrochemically Switchable [2]Catenane Incorporating a Tetrathiafulvalene Unit. *Angew. Chem., Int. Ed.* **1998**, *37*, 333–337.
- 44 Nygaard, S.; Leung, K. C.-F.; Aprahamian, I.; Ikeda, T.; Saha, S.; Laursen, B. W.; Kim, S.-Y.; Hansen, S. W.; Stein, P. C.; Flood, A. H.; Stoddart, J. F.; Jeppesen, J. O. Functionally Rigid Bistable [2]Rotaxanes. *J. Am. Chem. Soc.* **2007**, *129*, 960–970.
- 45 Ballardini, R.; Balzani, V.; Dehaen, W.; Dell'Erba, A. E.; Raymo, F. M.; Stoddart, J. F.; Venturi, M. Anthracene-Containing [2]Rotaxanes: Synthesis, Spectroscopic, and Electrochemical Properties. *Eur. J. Org. Chem.* **2000**, *4*, 591–602.
- 46 Trabolsi, A.; Fahrenbach, A. C.; Dey, S. K.; Share, A. I.; Friedman, D. C.; Basu, S.; Gasa, T. B.; Khashab, N. M.; Saha, S.; Aprahamian, I.; Khatib, H. A.; Flood, A. H.; Stoddart, J. F. A Tristable [2]Pseudo[2]Rotaxane. *Chem. Commun.* **2010**, *46*, 871–873.
- 47 Jeppesen, J. O.; Nielsen, K. A.; Perkins, J.; Vignon, S. A.; Di Fabio, A.; Ballardini, R.; Gandolfi, M. T.; Venturi, M.; Balzani, V.; Becher, J.; Stoddart, J. F. Amphiphilic Bistable Rotaxanes. *Chem.—Eur. J.* **2003**, *9*, 2982–3007.
- 48 Amabilino, D. B.; Ashton, P. R.; Boyd, S. E.; Gómez-López, M.; Hayes, W.; Stoddart, J. F. Translational Isomerism in Some Two- and Three-Station [2]Rotaxanes. *J. Org. Chem.* **1997**, *62*, 3062–3075.
- 49 Cao, D.; Amelia, M.; Klivansky, L. M.; Koshakaryan, G.; Khan, S. I.; Semeraro, M.; Silvi, S.; Venturi, M.; Credi, A.; Liu, Y. Probing Donor-Acceptor Interactions and Co-Conformational Changes in Redox Active Desymmetrized [2]Catenanes. *J. Am. Chem. Soc.* **2010**, *132*, 1110–1122.
- 50 Ashton, P. R.; Ballardini, R.; Balzani, V.; Credi, A.; Dress, K. R.; Ishow, E.; Kleverlaan, C. J.; Kocian, O.; Preece, J. A.; Spencer, N.; Stoddart, J. F.; Venturi, M.; Wenger, S. A. Photochemically Driven Molecular-Level Abacus. *Chem.—Eur. J.* **2000**, *6*, 3558–3574.
- 51 Olsen, J.-C.; Fahrenbach, A. C.; Trabolsi, A.; Friedman, D. C.; Dey, S. K.; Gothard, C. M.; Shveyd, A. K.; Gasa, T. B.; Spruell, J. M.; Olson, M. A.; Wang, C.; Jacquot de Rouville, H.-P.; Botros, Y. Y.; Stoddart, J. F. A Neutral Redox-Switchable [2]Rotaxane. *Org. Biomol. Chem.* **2011**, *9*, 7126–7133.
- 52 Coskun, A.; Saha, S.; Aprahamian, I.; Stoddart, J. F. A Reverse Donor-Acceptor Bistable [2]Catenane. *Org. Lett.* **2008**, *10*, 3187–3190.
- 53 Eliel, E. L. *Stereochemistry of Carbon Compounds*, McGraw-Hill: New York, 1962; pp 219–239.
- 54 Stoddart, J. F. *Stereochemistry of Carbohydrates*, John Wiley and Sons: New York, 1971; pp 58–92.